World Scientific
www.worldscientific.com

SILICON NANOPARTICLES/PEDOT−PSS NANOCOMPOSITE AS AN EFFICIENT COUNTER ELECTRODE FOR DYE-SENSITIZED SOLAR CELLS

DANDAN SONG*, MEICHENG LI*,†,‡, FAN BAI*, YINGFENG LI*,
YONGJIAN JIANG* and BING JIANG*

*State Key Laboratory of Alternate Electrical Power System with Renewable Energy Sources
North China Electric Power University, Beijing 102206, P. R. China

†Suzhou Institute, North China Electric Power University, Suzhou 215123, P. R. China
‡mcli@ncepu.edu.cn

A novel inorganic/organic nanocomposite film composed of Si nanoparticles (NPs) and poly-(3,4-ethylenedioxythiophene)-poly (styrenesulfonate) (PEDOT−PSS) is obtained from a simple mechanical mixture of Si NPs powder and aqueous PEDOT−PSS solution. Employing this composite film as a counter electrode, dye-sensitized solar cell (DSSC) exhibits an efficiency of 5.7% and a fill factor of 0.51, which are much higher than these of DSSC using pristine PEDOT−PSS electrode (2.9% and 0.25, respectively). The improvements in the photovoltaic performance of the former are primarily derived from improved electrocatalytic performance of the electrode, as evidenced by electrochemical measurements, the composite electrode has lower impedance and higher electrocatalytic activity when in comparison with pristine PEDOT−PSS electrode. These improvements are primarily deriving from the increased electrochemical surface by the addition of Si NPs. The characteristics of Si NPs/PEDOT−PSS composite counter electrode reveal its potential for the use of low-cost and stable Pt-free counter electrode materials. In addition, the results achieved in this work also provide a facile and efficient approach to improve the photovoltaic performance of DSSCs using PEDOT−PSS electrodes.

Keywords: Si nanoparticles; PEDOT−PSS; counter electrode; fill factor; dye sensitized solar cells.

Dye sensitized solar cells (DSSCs), presenting potentially low-cost fabrication and high conversion efficiencies, are considered to be promising alternatives for traditional inorganic solar cells.[1,2] In DSSC, a thin layer of Pt nanoparticles (NPs) deposited on FTO conducting glass is usually employed as the counter electrode (CE) which catalyzes the reduction of triiodide (I_3^-) in electrolyte.[3] However, the inevitable drawbacks of Pt CE including the corrosive character in presence of water [4,5] and the rarity of Pt materials, should be addressed before the large-scale application of DSSCs. Hence, the explorations of Pt-free CEs are attracting increased research interests,[6,7] and of which nano-carbon[4] and PEDOT[8] attract more interests. Poly-(3,4-ethylenedioxythiophene)-poly(styrenesulfonate) (PEDOT−PSS) is the only commercially available PEDOT polymer, exhibiting unique characteristics of low cost, facile and low temperature film fabrication, and high electronic conductivity.[9] However, DSSCs with PEDOT−PSS CEs yield poor fill factors (FFs) [less than 0.30 (see Ref. 6) and still exhibit much lower photoelectric conversion efficiencies than these of DSSCs with Pt CEs. In general, the low fill factor (FF) results from the high impedance in the charge transfer and/or redox couple diffusion processes, and the relative low electrocatalytic activity as compared with that of Pt CE.[10−13]

To solve these problems, one efficient route is using the composite of PEDOT−PSS and other functional materials, such as nanomaterials which possesses intrinsic large surface area and meanwhile effective electrocatalytic activity composed of inorganic metal compound semiconductors (CoS,[11] TiN,[12] CuInS,[13] etc). Despite of these reported materials incorporated with PEDOT−PSS, to enhance the electrocatalytic performance of PEDOT−PSS, and as well, simplify the preparation processes and reduce production cost, the exploration of more suitable nanomaterials are still crucial. Moreover, in these reported composite electrodes, the role of PEDOT−PSS is obscure, as these metal compound semiconductors individually exhibit Pt-like electrocatalytic properties and PEDOT−PSS seems to act as charge transport sites other than catalytic sites.

To get a further insight in the electrocatalytic property of PEDOT−PSS and meanwhile address the low FF problem in

DSSC, silicon NPs yielding poor electrocatalytic activity are incorporated with PEDOT−PSS through a simple preparation process. It is proved that the electrocatalytic activity of PEDOT−PSS can be notly increased just by increasing its surface area with the addition of Si NPs, which realizes high FF and efficiency when used as CE in DSSC.

Materials PEDOT−PSS aqueous solution (PH1000) and Si NPs (99.999%, 50 nm in mean diameter) were obtained from Clevios and Hefei Kaier Nano-meter Energy & Technology Co., China, respectively. TiO₂ NPs (P25) and N719 dye were acquired from Degussa and Dyesol, Australia, respectively. The I^-/I_3^- liquid electrolyte (DHS-E23), Pt/FTO and FTO glasses were purchased from Dalian HeptaChroma SolarTech Co., China.

Preparation of CE and DSSCs Si NPs/PEDOT−PSS nanocomposite solution was prepared by dispersing Si NPs powder in PEDOT−PSS solution, and then stirred and sonicated to form a well dispersed solution. The Si NPs/PEDOT−PSS composite and pristine PEDOT−PSS CEs were fabricated by spin-coating of their solutions on ozone-treated FTO-glass followed by a drying process at $120°C$. TiO₂ film was prepared by doctor-blading and calcinated at $450°C$ for 30 min, and after cooled to $80°C$, it was immersed in 3×10^{-4} M ethanol solution of N719 dye for 24 h. Then the dye-sensitized TiO₂ photoanode and the as-fabricated CEs were assembled together with $60\,\mu m$ thick Surlyn. Finally, the I^-/I_3^- liquid electrolyte with acetonitrile as the solvent was then injected between the two electrodes.

Characterization The current density−voltage curves of DSSCs were measured with a Keithley 2400 source meter under $100\,mW/cm^2$ irradiation from a solar simulator (XES-301S + EL − 100). SEM images were acquired using a FEI Quanta 200F field emission electron microscope. The electrochemical impedance spectroscopy (EIS) and Tafel curves were obtained using the electrochemical workstation (CHI660D). The frequency varied from 100 kHz to 0.1 Hz.

Photovoltaic performance of DSSCs The photocurrent density−voltage (J−V) curves of DSSCs employing various CEs are shown in Fig. 1, and their photovoltaic parameters are summarized in Table 1. DSSC equipped with pristine PEDOT−PSS CE yields a FF of 0.25 and a photoelectric conversion efficiency (PCE) of 2.9%, as in accordance with the typical scales reported in previous literatures.[11−13] With the addition of Si NPs in PEDOT−PSS, the FF of related DSSC increases consistently with the amounts of Si NPs. In consequence, the PCE also increases to the highest value of 5.7%, which nearly double that with pristine PEDOT−PSS. DSSC equipped Pt CE shows a FF of 0.59 and a PCE of 6.6%. In addition, DSSC with pristine Si NPs CE has been fabricated, which shows bad performance with a FF of 0.09 and a PCE of 0.1%, implying that Si NPs individually possess poor catalytic activity for I_3^- reduction.
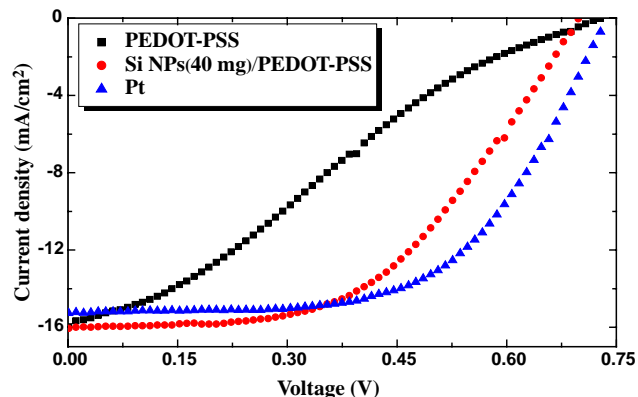

Fig. 1. Current density−voltage curves of DSSCs employing various counter electrodes under $100\,mW/cm^2$ irradiation condition.

Table 1. The photovoltaic parameters of DSSCs with various CEs.

CEs	V_{OC} (V)	J_{SC} (mA/cm²)	FF	PCE (%)
PEDOT−PSS	0.73	15.96	0.25	2.9
Si NPs (5 mg)/PEDOT−PSS	0.70	17.06	0.37	4.4
Si NPs (40 mg)/PEDOT−PSS	0.70	16.05	0.51	5.7
Pt	0.73	15.26	0.59	6.6

From J−V results, it is clear that the improved PCE of DSSC with Si NPs/PEDOT−PSS CE primarily due to the increased FF, which mainly differs in the voltage below 0.4 V. As shown in Fig. 1, the decrease of current density with increasing voltage is quite sharp when using PEDOT−PSS CE, and becomes moderate in condition of Si NPs/PEDOT−PSS CE. In this voltage scale, the electronic transport is supposed to be dominated by catalytic reaction at the CE/electrolyte interface,[14] which can be investigated by EIS.

Electrochemical properties EIS is employed to investigate the variations in the catalytic reactions associated with the CE configurations.[10,15] Figure 2(a) represents the Nyquist plots from PEDOT−PSS, Si NPs (40 mg)/PEDOT−PSS and Pt CEs and the equivalent circuit of DSSC. The total impedance is high when using PEDOT−PSS CE (larger than $180\,\Omega$), while is less than $90\,\Omega$ and $50\,\Omega$ when using Si NPs/PEDOT−PSS composite CE and Pt CE, respectively. The trend in the change of the total impedance of these three DSSCs agrees well with that of their photovoltaic performance, that is, lower impedance leads to larger FF and higher PCE. The simulated results by fitting the experimental spectra with the equivalent circuit using Zsim are summarized in Table 2. R_S represents for the series resistance at electrode/FTO contact, while R_{ct1} and R_{ct2} represents for the charge transfer resistance at CE interface and TiO₂ interface, respectively.[11,16] The component Z_{W1} associates with the Nernst diffusion impedance of I_3^-/I^- redox couple in the electrolyte, and Z_{W2} associates with the diffusion impedance
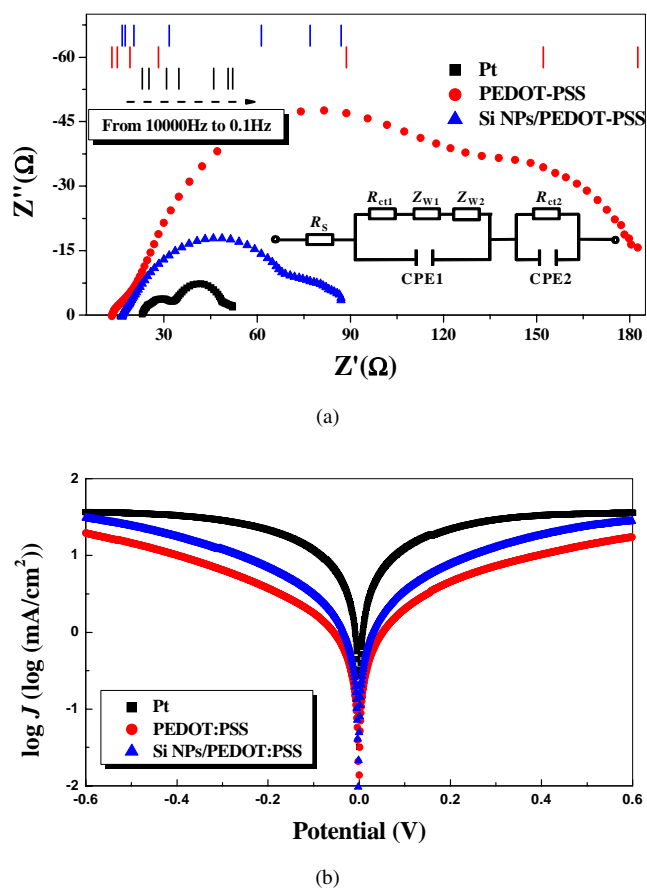
(a)

Fig. 2. (a) Nyquist spectra from DSSCs using various CEs, and (b) Tafel polarization curves from dummy cells using various CEs. The scale bars inset (a) represents for the frequencies of 10 k to 0.1 Hz, and the different colors represent different CEs.
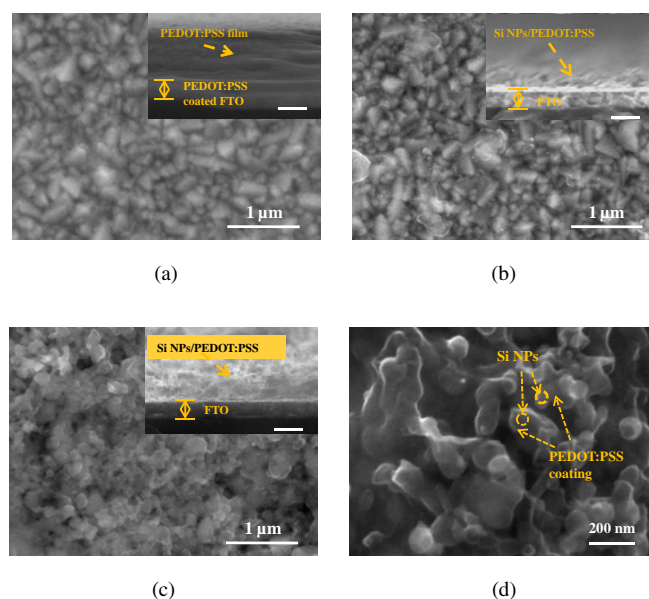

Fig. 3. The SEM images from various films on FTO glasses, (a) PEDOT−PSS film, (b) Si NPs (5 mg)/PEDOT−PSS film, (c) Si NPs (40 mg)/PEDOT−PSS film and (d) the magnification image of Si NPs (40 mg)/PEDOT−PSS film. The insets are the corresponding cross-sectional images of these films, the scale bars in which represent for 1 μm.

of I_3^-/I^- in porous electrode and thus is not included in Pt CE. It is clear that all the impedances associated with CE (R_{ct1}, Z_{W1} and Z_{W2}) are reduced with the presence of Si NPs in PEDOT−PSS CE. Furthermore, in comparison with Pt CE, the higher Z_{W1} and Z_{W2} in PEDOT−PSS based CEs illustrate that, the I^-/I_3^- diffusion process is the main origin for the changes in the electrocatalytic effect and photovoltaic performances employing various CEs.

Tafel polarization curves are also characterized using a symmetric sandwich cell consisting of two identical CEs, as shown in Fig. 2(b). The exchanged current density (J_0), which reflects the electrocatalytic ability of an electrode, can be estimated from the extrapolated intercepts of the anodic and cathodic branches of the corresponding Tafel curves.[17,18] The composite CE shows an increased J_0 than pristine

Table 2. Electrochemical impedance of DSSCs with various CEs.

CEs	R_S (Ω)	R_{ct1} (Ω)	R_{ct2} (Ω)	Z_{W1} (Ω)	Z_{W2} (Ω)
PEDOT−PSS	13.15	4.75	40.02	78.65	51
Si NPs/PEDOT−PSS	16.81	1.98	34.27	33.39	6
Pt	23.06	10.33	12.96	7.66	/

PEDOT−PSS CE, indicating that the electrocatalytic of PEDOT−PSS CE has been improved by some extent with the presence of Si NPs. It has been observed that J_0 is largest in Pt CE, which is conflict with its large R_{ct1} value, probably due to the differences in polarization process between metal and porous semiconductor electrodes.

Film morphology As Si NPs exhibits poor catalytic activity, the improved electrocatalytic property in Si NPs/PEDOT−PSS CE is probably due to the enlarged effective electrochemical surface area. The scanning electron microscopy (SEM) technique is employed to study the structural features, and the images are shown in Fig. 3. In pristine PEDOT−PSS film (Fig. 3(a)), the cross-sectional view clearly shows that the film is rough and compact with a thickness of several tens of nanometer, and hence, the effective electrocatalytic surface area is limited. With the presence of a small amount of Si NPs (5 mg) in PEDOT−PSS film (Fig. 3(b)), the roughness increases and the film become porous. The porous feature is more obvious with 40 mg Si NPs in PEDOT−PSS film, as evidenced by SEM images shown in Fig. 3(c). The film thickness is also increased (1−2 μm). The magnification SEM image of Si NPs/PEDOT−PSS film (Fig. 3(d)) reveals that Si NPs are coated and connected by PEDOT−PSS. Hence, the effective electrochemical surface area, which is expected to be responsible for the increased electrocatalytic activity of CEs,[10,19,20] has been increased with the presence of Si NPs.

The mechanisms Based on the above results, the catalytic mechanism of Si NPs/PEDOT−PSS composite towards I_3^- reduction is depicted in Fig. 4. In pristine PEDOT−PSS CE,

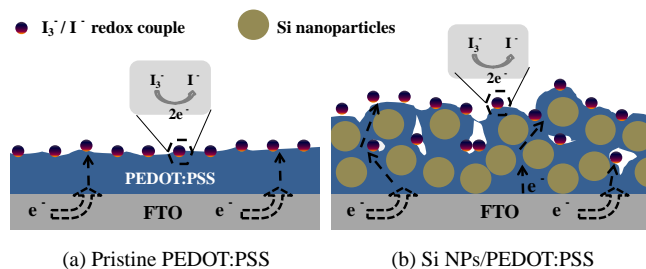(a) Pristine PEDOT:PSS

(b) Si NPs/PEDOT:PSS

Fig. 4.   Schematic of the catalytic mechanisms of (a) pristine PEDOT−PSS and (b) Si NPs/PEDOT−PSS CEs.

the large size of the dopant PSS chains impedes the contacts or interactions between active sites of PEDOT chains and I_3^-/I^-,[11] and its dense morphology prevents the penetrating of I_3^- in PEDOT−PSS film, resulting in the weak catalytic effect on I_3^- reduction. When Si NPs are added in PEDOT−PSS film, the formed porous morphology, as shown in SEM images, facilitates the diffusion of I_3^- species into the electrode (which reduces the diffusion impedance as proved by EIS results), and promotes high numbers of PEDOT−PSS chains exposed to redox couples. Hence, the active sites of PEDOT towards I_3^- reduction will be increased, as evidenced by the increased exchange current in Tafel curves. Therefore, the Si NPs/PEDOT−PSS composite CE presents enhanced catalytic effect toward I_3^- reduction and thus a high FF when used as CE in DSSC. In addition, the connection of PEDOT−PSS outside Si NPs enables efficient charge transport in electrode via high conductive PEDOT−PSS sites.

The interface of FTO/CE also plays a crucial role in determining FF values per some stuides.[21] Hence, the potential effect of FTO/CE interface was investigated by employing double layered CE construction with an ultra thin layer at FTO side and a normal layer at the electrolyte side. The ultra thin layer is obtained at a high spin-coating speed (7000 rpm, while 1000 rpm for normal layers), and is expected to provide only a functional interface (FTO/CE) but little effect on electrolyte reduction or charge transport in CE. The J−V
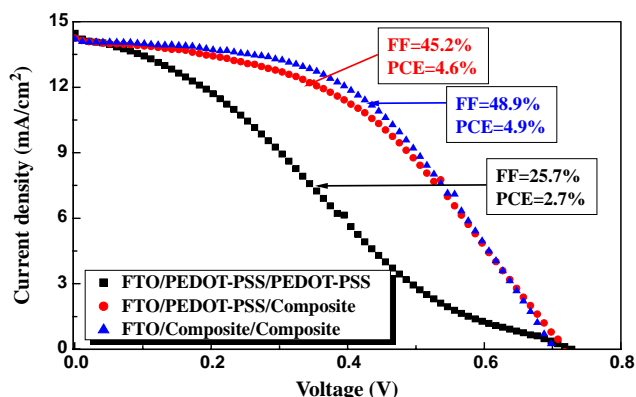
curves from these DSSCs provided in Fig. 5 show that, the use of composite CE contacting with electrolyte increases the FF and PCE of the related DSSCs obviously, while further use of composite CE contacting with FTO side affects little on FF and PCE. These results suggest that the introduction of Si NPs in CEs primarily affects the active sites of CEs toward electrolyte.

In summary, Si NPs/PEDOT−PSS nanocomposite film is explored for the use of efficient CE in DSSCs through a simple mechanical mixture of Si NPs and PEDOT−PSS followed by spin-coating on FTO glass. This composite electrode exhibits effective electrocatalytic activity for I_3^- reduction. In consequence, DSSC using this composite as CE yields comparable photovoltaic performance with that using Pt electrode, while much better than that using pristine PEDOT−PSS electrode. This work provides an efficient and facile approach to improve the performance of DSSCs using PEDOT−PSS electrode. Furthermore, the preparation at low temperatures of Si NPs/PEDOT−PSS electrode and the low cost of Si NPs present its potential in flexible and large scale applications.

Acknowledgment

References

1. M. Grätzel, *Acc. Chem. Res.* **42**, 1788 (2009).
2. B. E. Hardin *et al.*, *Nat. Photon.* **6**, 162 (2012).
3. A. Hagfeldt *et al.*, *Chem. Rev.* **110**, 6595 (2010).
4. A. Kay and M. Grätzel, *Sol. Energy Mater. Sol. Cells* **44**, 99 (1996).
5. G. Syrrokostas *et al.*, *Sol. Energy Mater. Sol. Cells* **103**, 119 (2012).
6. J. Xia and S. Yanagida, *Solar Ener.* **85**, 3143 (2011).
7. M. Wu *et al.*, *J. Am. Chem. Soc.* **134**, 3419 (2012).
8. Y. Saito *et al.*, *Chem. Lett.* **31**, 1060 (2002).
9. Y. Wang, *J. Phys.: Conf. Ser.* **152**, 012023 (2009).
10. G. Yue *et al.*, *J. Phys. Chem. C* **116**, 18057 (2012).
11. P. Sudhagar *et al.*, *ACS Appl. Mater. Interfaces* **3**, 1838 (2011).
12. H. Xu *et al.*, *ACS Appl. Mater. Interfaces* **4**, 1087 (2012).
13. Z. Zhang *et al.*, *ACS Appl. Mater. Interfaces* **4**, 6242 (2012).
14. G. Kron *et al.*, *Electrochem. Solid-State Lett.* **6**, E11 (2003).
15. Q. Wang *et al.*, *J. Phys. Chem. B* **109**, 14945 (2005).
16. J. Song *et al.*, *J. Mater. Chem.* **22**, 20580 (2012).
17. C. W. Kung *et al.*, *ACS Nano* **6**, 7016 (2012).
18. A. J. Bard and L. R. Faulkner, *Electrochemical Methods: Fundamentals and Applications*, 2nd edn. (John Wiley & Sons Inc., New York, 2000), pp. 103−104.
19. M. Y. Yen *et al.*, *RSC Adv.* **2**, 2725 (2012).
20. S. J. Peng *et al.*, *J. Mater. Chem.* **22**, 5308 (2012).
21. J. Xia *et al.*, *J. Mater. Chem.* **17**, 2845 (2007).

Fig. 5.   Current density−voltage curves of DSSCs using various double counter electrodes under 100 mW/cm^2 irradiation condition.